Contribution from the Department of Chemistry and Molecular Structure Center, Indiana University, Bloomington, Indiana 47405, and Department of Chemistry, University of California at San Diego, La Jolla, California 92093-0506

Preparation and Properties of the Triply Bridged, Ferromagnetically Coupled Dinuclear Copper(II) Complexes [Cu₂(OAc)₃(bpy)₂](ClO₄) and [Cu₂(OH)(H₂O)(OAc)(bpy)₂](ClO₄)₂

George Christou,*[1a] Spiros P. Perlepes,[1a,d] Eduardo Libby,[1a] Kirsten Folting,[1b] John C. Huffman,[1b] Robert J. Webb,[1c] and David N. Hendrickson*[1c]

A systematic investigation of the reactions between $Cu_2(O_2CMe)_4(H_2O)_2$ with 2,2'-bipyridine (bpy) has been initiated, and initial results are described. Treatment of $Cu_2(O_2CMe)_4(H_2O)_2$ with 2 equiv of bpy and $NaClO_4$ in EtOH yields $[Cu_2(O_2CMe)_3(bpy)_2](ClO_4)$ (**1a**) in 95% yield. The PF_6^- salt (**1b**) can be prepared similarly. Treatment of the reaction solution to **1a** with 1 equiv of NaOH prior to addition of $NaClO_4$ leads to the high-yield precipitation of the known compound $Cu_2(OH)_2(bpy)_2(ClO_4)_2$ (**2**); from the filtrate slowly crystallized **1a** in 32% yield. If the amount of NaOH is doubled, essentially quantitative formation of complex **2** results. The same $Cu_2(O_2CMe)_4(H_2O)_2$/bpy/$NaClO_4$ reaction mixture in hot H_2O yields instead $[Cu_2(OH)(H_2O)(O_2CMe)(bpy)_2](ClO_4)_2$ (**3**) in ~70% yield. Complex **1a** has been found to undergo facile carboxylate substitution when the more acidic PhCOOH is added; addition of excess PhCOOH to **1a** in MeCN or MeOH leads to essentially quantitative yields of $[Cu_2(O_2CPh)_3(bpy)_2](ClO_4)$ (**4**). Complex **1a** crystallizes in triclinic space group $P\bar{1}$ with, at -154 °C, $a = 11.973$ (2) Å, $b = 18.576$ (4) Å, $c = 7.745$ (1) Å, $\alpha = 103.96$ (1)°, $\beta = 65.92$ (1)°, $\gamma = 119.58$ (0)°, and $Z = 2$. A total of 3271 unique data with $F > 2.33\sigma(F)$ were refined to values of R and R_w of 2.57 and 2.21%, respectively. Complex **3** crystallizes in triclinic space group $P\bar{1}$ with, at -160 °C, $a = 11.286$ (2) Å, $b = 16.414$ (4) Å, $c = 8.047$ (2) Å, $\alpha = 97.31$ (1)°, $\beta = 103.78$ (1)°, $\gamma = 72.59$ (1)°, and $Z = 2$. A total of 3079 unique data with $F > 3.00\sigma(F)$ were refined to values of R and R_w of 4.67 and 4.86%, respectively. The structure of **1a** consists of a dinuclear $[Cu_2(O_2CMe)_3(bpy)_2]^+$ cation with three acetate bridges and a well-separated anion. Two of the acetates are in the familiar bidentate $\eta^1:\eta^1:\mu_2$ bridging mode, and the third is in the rarer monoatomic bridging mode; a terminal bpy molecule completes five-coordination at each metal atom. There is evidence for an additional weak interaction between one of the Cu^{II} atoms and the uncoordinated oxygen of the monoatomic bridging acetate group (Cu⋯O = 2.716 (2) Å). The coordination geometries of the two Cu^{II} atoms are significantly different. One Cu^{II} possesses square-pyramidal geometry, while the other is closer to being trigonal bipyramidal. The structure of the cation of complex **3** consists of a triply (OH⁻, H_2O, $MeCO_2^-$) bridged pair of five-coordinate copper atoms. The acetate group is in the bidentate $\eta^1:\eta^1:\mu_2$ bridging mode; a terminal bpy molecule completes five-coordination at each metal. The metal coordination geometries are best described as square pyramidal with the water oxygen occupying the apical positions of both metals. The cations of **3** form infinite chains as a result of H-bonding interactions with the ClO_4^- anions. The results of solid-state magnetic susceptibility studies are described for complexes **1a** and **3** in the temperature range 5-300 K. The results reveal intramolecular ferromagnetic coupling in both complexes. Fitting parameters are $J = +3.6$ cm⁻¹, $g = 2.1$, and $\theta = 0.20$ K for **1a** and $J = +19.3$ cm⁻¹, $g = 2.1$, and $\theta = 4.5$ K for **3**. The magnetic properties can be explained by considering the orbital pathways that are available for exchange, the symmetry of the copper magnetic orbitals, and noncomplementary orbital effects. An electrochemical study of **1a** in MeCN reveals a quasi-reversible two-electron reduction at -0.74 V vs ferrocene and an irreversible two-electron reduction at $E_p = -1.80$ V, yielding Cu metal that deposits on the electrode. Controlled-potential coulometry shows that the two-electron-reduced (Cu^I_2) form slowly disproportionates to Cu^{II}_2 and Cu metal. Complex **4** displays similar two-electron processes. Complex **3** gave only a very irreversible and poorly defined electrochemical response.

Introduction

Continuing interest in the synthesis and characterization of dinuclear copper(II) complexes draws from three quarters. First, there is a need to understand the factors that are responsible for the magnetic exchange interactions between coupled copper centers. Empirical structural/magnetic relationships (particularly involving bis(μ-hydroxo), bis(μ-alkoxo)-, and bis(μ-chloro)-bridged compounds and also μ-carboxylato complexes) have shown interesting correlations.[2] The type (antiferromagnetic or ferromagnetic) and magnitude of magnetic exchange interactions depend on the bridge identity, the M⋯M separation, the bond angles at the bridging atoms, the dihedral angle between the planes containing the copper(II) ions, the metal-bridge ligand bond lengths, and the metal ion stereochemistry.[2] However, while considerable advances have been made in understanding the relationships between structural features and the values of the magnetic exchange interaction constant, J, in symmetrical dibridged copper(II) dimers, the same degree of understanding has not yet been achieved for asymmetrical dibridged systems and triply bridged dimers. Second, there is a widespread occurrence

of dinuclear copper centers in biology.[3] In particular, the occurrence of a pair of copper ions at the active site of the various forms of the oxygen carrier protein hemocyanin in many species of arthropods and mollusks has stimulated much interest in modeling the active-site structure, physicochemical properties, and function of this protein by the use of model complexes.[4] Third, dinuclear copper(II) complexes are very promising candidates for the development of a new class of anion-exchangeable layer-structured compounds.[5]

Dinuclear copper(II) acetate complexes have been extremely useful for the study of intramolecular magnetic exchange interactions, mainly because the phenomenon was first recognized[2] in copper(II) acetate hydrate, a molecule that has been subjected to a large number of experimental and theoretical studies. Numerous copper(II) acetate adducts have been isolated and their magneto-structural correlations studied.[2b,d,f] In most cases, the formula of the complexes is $Cu_2(O_2CMe)_4L_2$; there are four bidentate bridging acetates and two monodentate ligands L occupying the axial positions. This type of acetate bridging normally

(1) (a) Indiana University Chemistry Department. (b) Indiana University Molecular Structure Center. (c) University of California at San Diego. (d) On sabbatical leave from the University of Ioannina, Ioannina, Greece.

(2) For review see: (a) Hodgson, D. J. *Prog. Inorg. Chem.* **1975**, *19*, 173. (b) Doedens, R. J. *Ibid.* **1976**, *21*, 209. (c) Kahn, O. *Comments Inorg. Chem.* **1984**, *3*, 105. (d) Melnik, M. *Coord. Chem. Rev.* **1982**, *42*, 259. (e) Kahn, O. *Angew. Chem., Int. Ed. Engl.* **1985**, *24*, 834. (f) Kato, M.; Muto, Y. *Coord. Chem. Rev.* **1988**, *92*, 45.

(3) (a) Solomon, E. I. In *Copper Proteins*; Spiro, T. G., Ed.; Wiley: New York, 1981; p 41. (b) Solomon, E. I.; Penfield, K. W.; Wilcox, D. E. *Struct. Bonding (Berlin)* **1983**, *53*, 1.

(4) (a) Patch, M. G.; Choi, H.-K.; Chapman, D. R.; Bau, R.; McKee, V.; Reed, C. A. *Inorg. Chem.* **1990**, *29*, 119 and references therein. (b) Tyklár, Z.; Karlin, K. D. *Acc. Chem. Res.* **1989**, *22*, 241. (c) Kitajima, N.; Fijisawa, K.; Moro-oka, Y. *J. Am. Chem. Soc.* **1989**, *111*, 8975. (d) Pate, J. E.; Ross, P. K.; Thamann, T. J.; Reed, C. A.; Karlin, K. D.; Sorrell, T. N.; Solomon, E. I. *J. Am. Chem. Soc.* **1989**, *111*, 5198 and references therein.

(5) Yamanaka, S.; Sako, T.; Hattori, M. *Chem. Lett.* **1989**, 1869.

results in substantial antiferromagnetic exchange interactions between the copper(II) atoms. Only a few attempts have been made to incorporate chelating ligands, instead of monodentate ones, into the $Cu_2(O_2CMe)_4$ structural unit.[6-9] In all cases, dimeric complexes with a smaller number of acetate ligands and interesting structural and magnetic characteristics have been obtained. A matter of interest is how much versatility and reactivity there is in the type of bridging found in copper(II) acetate and whether other small bridging ligands can be incorporated together with acetate bridges in the same complex.[9] For example, if dinuclear complexes containing both acetates and other bridging ligands form readily, then this finding would support a proposed mechanism whereby copper(II) acetate, acting as a template, can distinguish between ribo- and deoxyribonucleosides.[12]

As an extension to our studies of $Mn/RCO_2^-/bpy$ chemistry[13] (bpy is 2,2'-bipyridine), we have begun to investigate the reaction of $Cu_2(O_2CMe)_4(H_2O)_2$ with chelating bpy. We have employed Cu:bpy ratios of 1:1 since a 1:2 ratio is known to produce mononuclear $[Cu(O_2CMe)(bpy)_2]^+$ complexes.[14] We have found that the $Cu_2(O_2CMe)_4$ unit can be converted to $[Cu_2(O_2CMe)_3]^+$- and $[Cu_2(OH)(H_2O)(O_2CMe)]^{2+}$-containing products. Herein are described the syntheses, structures, properties, and magnetochemistry of these products.

Experimental Section

Compound Preparation. $Cu_2(O_2CMe)_4(H_2O)_2$, 2,2'-bipyridine, benzoic acid, anhydrous $NaClO_4$, $NBu^n_4PF_6$, NaOH, and all solvents were used as received. All operations were performed under aerobic conditions.

$[Cu_2(O_2CMe)_3(bpy)_2](ClO_4)$ (1a). Method A. Solid $Cu_2(O_2CMe)_4$-$(H_2O)_2$ (1.00 g, 2.5 mmol) was slowly dissolved with stirring in a solution of bpy (0.78 g, 5.0 mmol) in EtOH (70 cm³). After approximately 15 min, a deep blue homogeneous solution was obtained, and to this was added a solution of $NaClO_4$ (0.61 g, 5.0 mmol) in EtOH (10 cm³). The undisturbed solution soon began to deposit well-formed, sky blue crystals. The flask was stored at ambient temperature overnight, and the crystals were collected by filtration, washed with EtOH and Et_2O, and dried in air. The yield was 1.70 g (95%). The product was recrystallized from $MeCN/Et_2O$. Anal. Calcd for $C_{26}H_{25}N_4O_{10}ClCu_2$: C, 43.61; H, 3.53; N, 7.83; Cu, 17.75. Found: C, 43.5; H, 3.5; N, 7.7; Cu, 17.3. IR data (KBr): 3117 (w), 3109 (w), 3082 (w), 2999 (w), 2930 (w), 1638 (s), 1601 (vs, b), 1576 (m), 1566 (sh), 1495 (s), 1474 (s), 1448 (vs), 1427 (m), 1402 (s), 1371 (m), 1337 (w), 1302 (s), 1281 (sh), 1254 (m), 1226 (w), 1179 (s), 1163 (s), 1091 (vs, b), 1072 (s), 1057 (s), 1032 (m), 1018 (m), 977 (w), 920 (m), 814 (m), 777 (vs), 772 (vs), 739 (m), 732 (vs), 675 (m), 658 (m), 650 (m), 638 (w), 621 (vs), 559 (w), 514 (w), 488 (w), 458 (w), 443 (m), 421 (s), 418 (s), 405 cm⁻¹ (w). Solid-state (diffuse

reflectance) electronic spectrum (λ_{max}, nm): 361, 737 (sh), 746 (sh), 767, 791 (sh), 798 (sh), 836 (sh). Electronic spectrum [λ_{max}, nm (ϵ_M/Cu_2, L mol⁻¹ cm⁻¹): in MeCN, 686 (120); in CH_2Cl_2, 706 (120).

Method B. $Cu_2(O_2CMe)_4(H_2O)_2$ (1.00 g, 2.5 mmol) and bpy (0.78 g, 5.0 mmol) were dissolved in EtOH (50 cm³). The resulting deep blue solution was stirred while solid NaOH (0.10 g, 2.5 mmol) was added to give a darker blue homogeneous solution. Addition of a solution of $NaClO_4$ (0.68 g, 5.5 mmol) in EtOH (20 cm³) yielded immediately a lavender powder of the known[15] compound $Cu_2(OH)_2(bpy)_2(ClO_4)_2$ (2), which was collected by filtration, washed copiously with EtOH (not added to the filtrate), and dried in vacuo; yield 0.76 g (45% based on total available Cu). Anal. Calcd for $C_{20}H_{18}N_4O_{10}Cl_2Cu_2$: C, 35.72; H, 2.70; N, 8.33; Cu, 18.90. Found: C, 36.0; H, 2.8; N, 8.1; Cu, 18.4. The identity of this product was also confirmed by IR and electronic spectral comparison with authentic material.[15a] Overnight storage of the flask containing the filtrate at ambient temperature yielded sky blue crystals of **1a**, which were collected by filtration, washed with EtOH and Et_2O, and dried in air; yield 0.56 g (32% based on total available Cu). The IR and electronic spectra of this material were identical with those detailed under method A. Using 0.20 g (5.0 mmol) of NaOH, the above synthetic procedure yielded complex **2** in a nearly quantitative yield.

$[Cu_2(O_2CMe)_3(bpy)_2](PF_6)$ (1b). $Cu_2(O_2CMe)_4(H_2O)_2$ (1.00 g, 2.5 mmol) and bpy (0.78 g, 5.0 mmol) were dissolved in EtOH (50 cm³). To the resulting deep blue solution was added a solution of $NBu^n_4PF_6$ (1.90 g, 5.0 mmol) in MeCN (20 cm³). The homogeneous solution obtained was allowed to stand undisturbed at ambient temperature overnight, and the resulting sky blue crystals were collected by filtration, washed with THF and Et_2O, and dried in vacuo; yield 0.78 g (41%). Recrystallization can be effected from $MeCN/Et_2O$. The IR feature at 3439 cm⁻¹ assignable to H_2O suggested the dried solid to be hygroscopic, and this was supported by the analytical data, which gave a reasonable fit for [Cu_2-$(O_2CMe)_3(bpy)_2](PF_6)\cdot H_2O$. Anal. Calcd for $C_{26}H_{27}N_4O_7PF_6Cu_2$: C, 40.05; H, 3.50; N, 7.19; P, 3.97; Cu, 16.30. Found: C, 39.7, H, 3.5; N, 7.3; P, 4.1; Cu, 16.0. IR data (KBr): 3439 (w, b), 3117 (w), 3090 (w), 3040 (w), 2986 (w), 1641 (s), 1604 (s), 1593 (vs, b), 1569 (sh), 1496 (s), 1474 (s), 1449 (vs), 1428 (s), 1406 (s), 1369 (m), 1348 (m), 1308 (vs), 1281 (sh), 1268 (w), 1252 (m), 1222 (w), 1179 (m), 1163 (s), 1122 (w), 1109 (w), 1073 (w), 1059 (m), 1046 (m), 1034 (s), 1019 (m), 977 (w), 925 (m), 906 (w), 844 (vs, b), 812 (m), 769 (vs), 763 (s), 742 (m), 731 (s), 678 (m), 671 (m), 659 (m), 651 (m), 638 (m), 614 (m), 558 (vs), 490 (w), 442 (w), 418 (s), 409 cm⁻¹ (w). Solid-state (diffuse reflectance) electronic spectrum (λ_{max}, nm): 353 (sh), 725 (sh), 745, 770 (sh), 795 (sh), 840 (sh).

$[Cu_2(OH)(H_2O)(O_2CMe)(bpy)_2](ClO_4)_2$ (3). Method A. To a solid mixture containing $Cu_2(O_2CMe)_4(H_2O)_2$ (1.00 g, 2.5 mmol), bpy (0.78 g, 5.0 mmol), and $NaClO_4$ (0.61 g, 5.0 mmol) was added EtOH (10 cm³). To the resulting slurry was added H_2O (65 mL). The mixture was heated to 75 °C and stirred for a few minutes to yield a deep blue homogeneous solution. After cooling and overnight storage at room temperature, the resulting well-formed blue needles were collected by filtration, washed with cold water, THF, and Et_2O, and dried in air; yield 1.27 g (69%). The product was recrystallized from boiling water. Anal. Calcd for $C_{22}H_{22}N_4O_{12}Cl_2Cu_2$: C, 36.07; H, 3.03; N, 7.65; Cu, 17.35. Found: C, 36.2; H, 2.95; N, 7.4; Cu, 17.7. IR data (KBr): 3535 (m), 3409 (m, b), 3116 (m), 3085 (m), 3069 (w), 3039 (w), 2934 (w), 1611 (m), 1603 (s), 1577 (s), 1555 (vs, b), 1497 (m), 1474 (s), 1448 (vs), 1322 (m), 1316 (m), 1310 (m), 1282 (w), 1268 (w), 1252 (m), 1222 (w), 1176 (m), 1116 (vs, b), 1074 (s), 1055 (s), 1031 (s), 1020 (sh), 982 (w), 928 (m), 901 (w), 811 (w), 773 (vs), 747 (w), 733 (s), 679 (m), 664 (m), 652 (m), 624 (s), 566 (m), 490 (m), 456 (m), 419 cm⁻¹ (s). Solid-state (diffuse reflectance) electronic spectrum (λ_{max}, nm): 355, 590, 625 (sh), 1115.

Method B. A slurry of complex **1a** (0.43 g, 0.6 mmol) in H_2O (10 cm³) was stirred at 50 °C for 20 min. After cooling of the blue solution to room temperature, the blue solid was collected by filtration, washed with cold H_2O, Me_2CO, and Et_2O, and dried in vacuo; yield 0.18 g (42% based on total available Cu). The product had IR and electronic spectra identical with those detailed under method A.

Method C. A slurry of complex **1a** (0.43 g, 0.6 mmol) in H_2O (10 cm³) was treated with solid $NaClO_4$ (0.08 g, 0.65 mmol). The reaction mixture was stirred for 10 min at room temperature, and the product was collected by filtration, washed with Me_2CO and Et_2O, and dried in vacuo; yield 0.37 g (84%). The product was identical with **3** on spectroscopic examination.

Method D. To a slurry of complex **2** (0.67 g, 1.0 mmol) in H_2O (16 cm³) was added glacial MeCOOH (0.06 mL, 1.0 mmol). A noticeable color change from lavender to blue occurred. The reaction mixture was

(6) (a) Butcher, R. J.; Overman, J. W.; Sinn, E. *J. Am. Chem. Soc.* **1980**, *102*, 3276. (b) Greenaway, A. M.; O'Connor, C. J.; Overman, J. W.; Sinn, E. *Inorg. Chem.* **1981**, *20*, 1508.

(7) Costes, J.-P.; Dahan, F.; Laurent, J.-P. *Inorg. Chem.* **1985**, *24*, 1018.

(8) Brown, S. J.; Tao, X.; Stephan, D. W.; Mascharak, P. K. *Inorg. Chem.* **1986**, *25*, 3377.

(9) Notable progress has been made by using binucleating ligands to model features of Cu_2 cores in hemocyanin and tyrosinase; during these efforts, a large number of dinuclear copper(II) complexes derived from binucleating ligands (which furnish the main bridging network) and containing also one[10] or two[11] "exogenous" bridging acetates have been structurally characterized and studied.

(10) Representative references: (a) Tolman, W. B.; Rardin, R. L.; Lippard, S. J. *J. Am. Chem. Soc.* **1989**, *111*, 4532 and references therein. (b) Nishida, Y.; Kida, S. *J. Chem. Soc., Dalton Trans.* **1986**, 2633. (c) Mazurek, W.; Kennedy, B. J.; Murray, K. S.; O'Connor, M. J.; Rodgers, J. R.; Snow, M. R.; Wedd, A. G.; Zwack, P. R. *Inorg. Chem.* **1985**, *24*, 3258. (d) Sorrell, T. N.; O'Connor, C. J.; Anderson, O. P.; Reibenspies, J. H. *J. Am. Chem. Soc.* **1985**, *107*, 4199. (e) McKee, V.; Zvagulis, M.; Dagdigian, J. V.; Patch, M. G.; Reed, C. A. *J. Am. Chem. Soc.* **1984**, *106*, 4765.

(11) Representative references: (a) Coughlin, P. K.; Lippard, S. J. *J. Am. Chem. Soc.* **1984**, *106*, 2328. (b) Bertoncello, K.; Fallon, G. D.; Hodgkin, J. H.; Murray, K. S. *Inorg. Chem.* **1988**, *27*, 4750.

(12) (a) Berger, N. A.; Tarien, E.; Eichhorn, G. L. *Nature (London), New Biol.* **1972**, *239*, 237. (b) Brun, G.; Goodgame, D. M. L.; Skapski, A. C. *Nature (London)* **1975**, *253*, 127. (c) Kirchner, S. J.; Fernardo, Q.; Chvapil, M. *Inorg. Chim. Acta* **1977**, *25*, L45.

(13) Christou, G. *Acc. Chem. Res.* **1989**, *22*, 328 and references therein.

(14) Hathaway, B. J.; Ray, N.; Kennedy, D.; O'Brien, N.; Murphy, B. *Acta Crystallogr., Sect. B* **1980**, *B36*, 1371.

(15) (a) McWhinnie, W. R. *J. Chem. Soc.* **1964**, 2959. (b) Toofan, M.; Bourshehri, A.; Ul-Haque, M. *J. Chem. Soc., Dalton Trans.* **1976**, 217.

Table I. Crystallographic Data for Complexes **1a** and **3**

param	1a	3
formula	$C_{26}H_{25}N_4O_{10}ClCu_2$	$C_{22}H_{22}N_4O_{12}Cl_2Cu_2$
M_r	716.05	732.43
space group	$P\bar{1}$	$P\bar{1}$
temp, °C	-154	-160
a, Å	11.973 (2)	11.286 (2)
b, Å	18.576 (4)	16.414 (4)
c, Å	7.745 (1)	8.047 (2)
α, deg	103.96 (1)	97.31 (1)
β, deg	65.92 (1)	103.78 (1)
γ, deg	119.58 (0)	72.59 (1)
V, Å^3	1365.95	1378.77
Z	2	2
ρ_{calc}, g cm^{-3}	1.741	1.764
λ, Å	0.710 69	0.710 69
μ, cm^{-1}	17.233	18.090
data colld	$6° \leq 2\theta \leq 45°$	$6° \leq 2\theta \leq 45°$
no. of obsd data	3271^a	3079^b
R, % (R_w, %)	2.57 (2.91)	4.67 (4.86)

$^a F > 2.33\sigma(F)$. $^b F > 3.00\sigma(F)$.

stirred for 1 h at 40 °C. The resulting blue solid was collected by filtration, washed with EtOH and Et$_2$O, and dried in vacuo; yield 0.53 g (72%). The identity of the product was deduced by IR spectral comparison with authentic material.

[Cu$_2$(O$_2$CPh)$_3$(bpy)$_2$](ClO$_4$) (4). Benzoic acid (0.25 g, 2.0 mmol) was dissolved in a stirred blue solution of complex **1a** (0.215 g, 0.3 mmol) in MeCN (35 cm^3). No noticeable color change occurred. Slow evaporation of solvent yielded well-formed turquoise crystals of **4**, which were collected by filtration, washed with Et$_2$O, and dried in air; yield 0.17 g (63%). Further addition of Et$_2$O to the filtrate yielded a second crop of microcrystals, which were isolated as above; overall yield 93%. Anal. Calcd for C$_{41}$H$_{31}$N$_4$O$_{10}$ClCu$_2$: C, 54.57; H, 3.47; N, 6.21; Cu, 14.08. Found: C, 54.4; H, 3.4; N, 6.3; Cu, 14.1. An analogous procedure employing MeOH as solvent gave the same product; the yield was essentially quantitative. IR data (Nujol): 3095 (w), 3065 (w), 1636 (m), 1624 (m), 1604 (sh), 1596 (s), 1573 (sh), 1563 (s), 1554 (sh), 1491 (m), 1435 (sh), 1402 (m), 1331 (m), 1309 (w), 1295 (w), 1274 (w), 1263 (w), 1247 (m), 1169 (m), 1163 (w), 1155 (w), 1133 (m), 1120 (m), 1089 (vs, b), 1064 (m), 1040 (w), 1033 (m), 1018 (m), 977 (m), 936 (m), 895 (w), 855 (w), 844 (m), 815 (w), 766 (s), 755 (s), 734 (sh), 725 (vs), 688 (w), 674 (m), 654 (m), 645 (w), 634 (m), 615 (s), 563 (w), 455 (m), 415 (m), 407 (m), 365 (w), 316 cm^{-1} (m). Solid-state (diffuse reflectance) electronic spectrum (λ_{max}, nm): 383, 710, 765, 830 (sh).

Reaction of 3 with NaOH. To a slurry of complex **3** (0.73 g, 1.0 mmol) in H$_2$O (6 cm^3) was added a solution of NaOH (0.04 g, 1.0 mmol) in H$_2$O (10 cm^3). A color change from blue to lavender occurred. The reaction mixture was stirred for 1 h and the precipitated solid collected by filtration, washed with EtOH and Et$_2$O, and dried in vacuo; yield 0.59 g (88%). The IR spectrum of the product was identical with that of complex **2**.

Reaction of 1a with NaOH and NaClO$_4$. To a slurry of complex **1a** (0.43 g, 0.6 mmol) in H$_2$O (10 cm^3) was added solid NaClO$_4$ (0.08 g, 0.65 mmol), followed by addition of a solution of NaOH (0.05 g, 1.25 mmol) in H$_2$O (5 cm^3). An immediate color change from blue to lavender occurred. The reaction mixture was stirred for 30 min, and the resulting solid was collected by filtration, washed with Me$_2$CO and Et$_2$O, and dried in vacuo; yield 0.37 g (92%). The product had an IR spectrum identical with that of compound **2**.

Caution! Perchlorate salts are potentially explosive. Although no detonation tendencies have been observed with **1a**, **3**, and **4**, caution is advised and handling of only small quantities is recommended.

X-ray Crystallography and Structure Solution. Data were collected on a Picker four-circle diffractometer at -154 and -160 °C for **1a** and **3**, respectively; details of the diffractometry, low-temperature facilities, and computational procedures employed by the Molecular Structure Center are available elsewhere.[16a] Data collection parameters are summarized in Table I. The structures were solved by a combination of direct methods (MULTAN) and Fourier techniques and refined by full-matrix least squares. For both complexes **1a** and **3**, a systematic search of a limited hemisphere of reciprocal space located a set of diffraction maxima with no symmetry or systematic absences, indicating a triclinic

space group. The choice of the centrosymmetric space group $P\bar{1}$ was confirmed by the successful solution and refinement of the structures.

For both complexes, all non-hydrogen atoms were readily located and refined with anisotropic thermal parameters. For **1a**, all hydrogen atoms were clearly visible in a subsequent difference Fourier map; for **3**, essentially all hydrogen atoms were located, including those from the OH$^-$ and H$_2$O groups. All hydrogen atoms were included in the final cycles and refined with isotropic thermal parameters. Final difference Fourier maps were essentially featureless, the largest peaks being 0.28 and 0.8 e/Å^3 for **1a** and **3**, respectively. Final discrepancy indices R and R_w are included in Table I.

Physical Measurements. Variable-temperature magnetic susceptibility data were measured by using a Series 800 VTS-50 SQUID susceptometer (SHE Corp.). The susceptometer was operated at a magnetic field strength of 10 kg. Diamagnetic corrections were estimated from Pascal's constants and subtracted from the experimental susceptibility data to obtain the molar paramagnetic susceptibilities of the compounds. These molar paramagnetic susceptibilities were fit to the appropriate theoretical expression by means of a least-squares-fitting computer program.[16b]
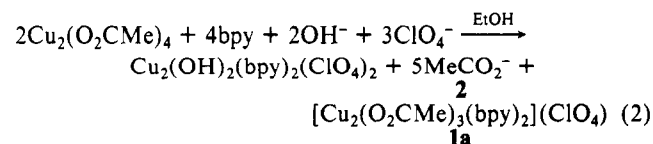
Elemental analyses were performed at the Microanalytical Laboratory, Department of Chemistry, Manchester University, Manchester, England. Infrared spectra were recorded as Nujol mulls or KBr disks by using a Nicolet 510P or Perkin-Elmer 283 spectrophotometer. Solid-state (diffuse reflectance, 1500–340 nm) and solution (800–400 nm) electronic spectra were recorded on a Perkin-Elmer 330 and Hewlett-Packard 4450A instruments, respectively. Cyclic voltammograms were recorded on an IBM Model EC 225 voltammetric analyzer and a PAR 175 universal programmer using a standard three-electrode assembly (glassy-carbon working, Pt-wire auxiliary, SCE reference) and 0.1 M NBu$^n_4$ClO$_4$ as supporting electrolyte. The scan rate was 100 mV/s, and no *IR* compensation was employed. Potentials are quoted versus ferrocene.

Results and Discussion

Syntheses and Reactivity Studies. In our development of Mn/O/RCO$_2^-$/bpy chemistry, we had employed to our advantage the fact that chelating bpy cannot be accommodated into, for example, the [Mn$_3$O(O$_2$CR)$_6$L$_3$]$^+$ unit without serious structural perturbation, resulting in a change in nuclearity to [Mn$_4$O$_2$-(O$_2$CR)$_7$(bpy)$_2$]$^+$. Our work with Cu was based on the same strategy; obviously bpy cannot be accommodated by the quadruply bridged Cu$_2$(O$_2$CMe)$_4$L$_2$ structure without serious change, and we reasoned that new types of bridged species might result (as long as the bpy:Cuy ratio was not high enough to lead to mononuclear products). This did, indeed, turn out to be the case. Treatment of Cu$_2$(O$_2$CMe)$_4$(H$_2$O)$_2$ with 2 equiv of bpy in EtOH followed by addition of NaClO$_4$ leads to essentially quantitative yields of [Cu$_2$(O$_2$CMe)$_3$(bpy)$_2$](ClO$_4$) (**1a**) possessing a novel type of triply bridged core. Its formation can be summarized in eq 1. The PF$_6^-$ salt **1b** can be prepared similarly. The presence of

$$Cu_2(O_2CMe)_4 + 2bpy + ClO_4^- \xrightarrow{\text{EtOH}}$$
$$\underset{\textbf{1a}}{[Cu_2(O_2CMe)_3(bpy)_2](ClO_4)} + MeCO_2^- \quad (1)$$
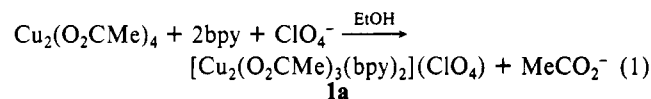
one monoatomic bridging acetate (vide infra) made us wonder whether it could be replaced by OH$^-$ to yield the [Cu$_2$(μ-OH)(μ-O$_2$CMe)$_2$]$^+$ core. We therefore treated the reaction solution to **1a** with 1 equiv of NaOH prior to addition of NaClO$_4$. The latter now gave a fine lavender precipitate of known Cu$_2$-(OH)$_2$(bpy)$_2$(ClO$_4$)$_2$ (**2**), which was collected by filtration after a few minutes (yield 45%); from the filtrate slowly crystallized **1a** in 32% yield. A reasonable rationalization of these observations is summarized in eq 2. Undoubtedly, a complex equilibrium
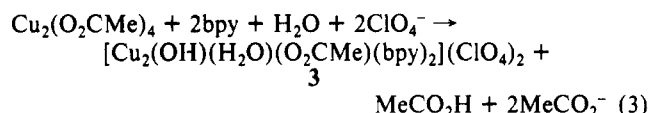
$$2Cu_2(O_2CMe)_4 + 4bpy + 2OH^- + 3ClO_4^- \xrightarrow{\text{EtOH}}$$
$$\underset{\textbf{2}}{Cu_2(OH)_2(bpy)_2(ClO_4)_2} + 5MeCO_2^- +$$
$$\underset{\textbf{1a}}{[Cu_2(O_2CMe)_3(bpy)_2](ClO_4)} \quad (2)$$

mixture is present in solution that is driven to formation of **2** by the insolubility of the latter.[17] Whether the intended product

(16) (a) Chisholm, M. H.; Folting, K.; Huffman, J. C.; Kirkpatrick, C. C. *Inorg. Chem.* **1984**, *23*, 1021. (b) Chandler, J. P. *Program 66*; Quantum Chemistry Program Exchange, Indiana University: Bloomington, IN.
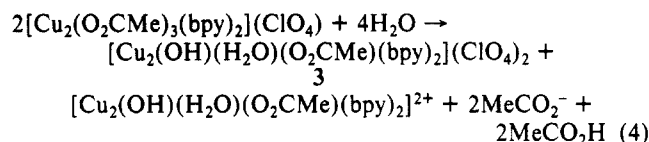
(17) We have now found that use of PF$_6^-$, instead of ClO$_4^-$, leads to a dramatic change in the identity of the products. Full details will be reported in due course.

cation $[Cu_2(OH)(O_2CMe)_2(bpy)_2]^+$ was present in solution is unclear; we are continuing to investigate this reaction. If the amount of NaOH is doubled, essentially quantitative formation of complex **2** results.
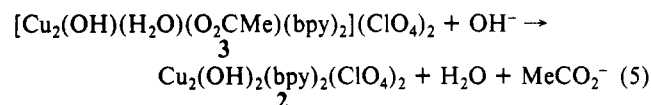
Foiled in our attempts to make a mixed-OH^-/$MeCO_2^-$-bridged Cu_2 complex with NaOH, we repeated the reaction in H_2O, hoping the less basic conditions would prevent formation of **2** and lead to the desired compound. The reaction mixture in H_2O (containing a little EtOH to aid dissolution of bpy) had to be heated before giving a homogeneous blue solution, and slow cooling gave beautiful blue crystals of $[Cu_2(OH)(H_2O)(O_2CMe)(bpy)_2](ClO_4)_2$ (**3**). This complex does have both OH^- and $MeCO_2^-$ bridges (vide infra) but only one of the latter, the third bridging ligand being a H_2O molecule. Its formation can be summarized in eq 3.

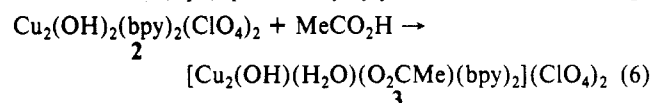$$Cu_2(O_2CMe)_4 + 2bpy + H_2O + 2ClO_4^- \rightarrow$$
$$\underset{\textbf{3}}{[Cu_2(OH)(H_2O)(O_2CMe)(bpy)_2](ClO_4)_2} +$$
$$MeCO_2H + 2MeCO_2^- \quad (3)$$

Since the reaction yields complexes **1a** and **3** if carried out in EtOH or H_2O, respectively, we suspected that **1a** would hydrolyze to **3** in H_2O; this was found to be the case in both cold and hot H_2O. Recrystallization of **1a** from warm water ($\sim$50 °C) yielded **3** in 42% yield based on Cu; the yield is ClO_4^--limited, however, as summarized in eq 4, and addition of $NaClO_4$ to the reaction

$$2[Cu_2(O_2CMe)_3(bpy)_2](ClO_4) + 4H_2O \rightarrow$$
$$\underset{\textbf{3}}{[Cu_2(OH)(H_2O)(O_2CMe)(bpy)_2](ClO_4)_2} +$$
$$[Cu_2(OH)(H_2O)(O_2CMe)(bpy)_2]^{2+} + 2MeCO_2^- +$$
$$2MeCO_2H \quad (4)$$

solution increases the yield of isolated **3** to 84%. It thus appears that complex **3** is the thermodynamically preferred product in aqueous solution (at $\sim$neutral pH). However, **3** will react in H_2O with NaOH (1 equiv) to yield complex **2** (88% isolated yield) as summarized in eq 5.   (Complex **1a** in H_2O containing NaOH

$$\underset{\textbf{3}}{[Cu_2(OH)(H_2O)(O_2CMe)(bpy)_2](ClO_4)_2} + OH^- \rightarrow$$
$$\underset{\textbf{2}}{Cu_2(OH)_2(bpy)_2(ClO_4)_2} + H_2O + MeCO_2^- \quad (5)$$

and $NaClO_4$ also gives **2** (92%) as expected.) This transformation of **3** to **2** is reversible; treatment of **2** with 1 equiv of acetic acid converts it to **3** (eq 6), presumably by protonation of a OH^- bridge

$$\underset{\textbf{2}}{Cu_2(OH)_2(bpy)_2(ClO_4)_2} + MeCO_2H \rightarrow$$
$$\underset{\textbf{3}}{[Cu_2(OH)(H_2O)(O_2CMe)(bpy)_2](ClO_4)_2} \quad (6)$$

followed by binding of the generated $MeCO_2^-$. Addition of excess acetic acid leads to a different product that has yet to be identified.

Finally, we anticipated that the complexes should be capable of carboxylate substitution on treatment with more acidic acids and have confirmed this for complex **1a**. Addition of excess benzoic acid to **1a** in MeCN or MeOH leads to essentially quantitative yields of $[Cu_2(O_2CPh)_3(bpy)_2](ClO_4)$ (**4**) (eq 7). This parallels the behavior observed for our $Mn/MeCO_2^-$/bpy complexes.[13]

$$[Cu_2(O_2CMe)_3(bpy)_2]^+ + 3PhCO_2H \rightarrow$$
$$\underset{\textbf{4}}{[Cu_2(O_2CPh)_3(bpy)_2]^+} + 3MeCO_2H \quad (7)$$
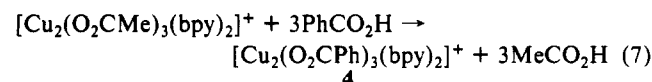
Description of Structures. The structures of the cations of complexes **1a** and **3** are shown in Figures 1 and 2, respectively. An ORTEP plot of the inner coordination sphere about the Cu_2 core for complex **3** is depicted in Figure 3, and a crystal packing diagram for the same complex is shown in Figure 4. Fractional coordinates for **1a** and **3** are listed in Tables II and III. Selected structural parameters for **1a** and **3** are listed in Tables IV and VI, respectively.

The structure of **1a** consists of a dinuclear $[Cu_2(O_2CMe)_3(bpy)_2]^+$ cation with three acetate bridges and a well-separated
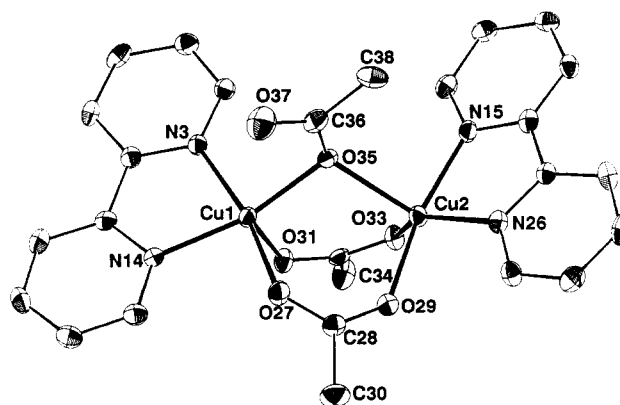
Figure 1. ORTEP representation of the cation of complex **1a** at the 50% probability level. Bipyridine carbon atoms are labeled consecutively from N3 and N15. The unlabeled carboxylate carbon atom is C32.
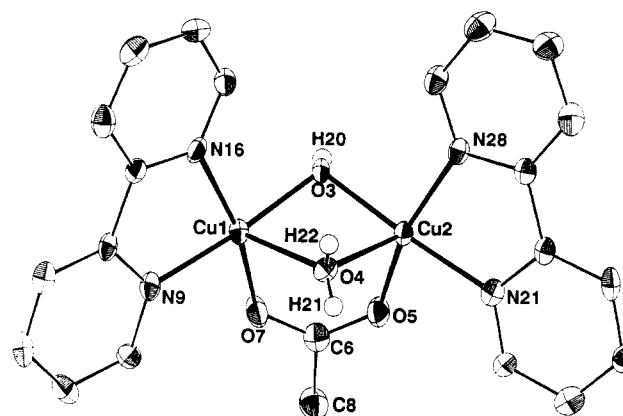

Figure 2. ORTEP representation of the cation of complex **3** at the 50% probability level. Bipyridine carbon atoms are labeled consecutively from N9 and N21. OH^- and H_2O hydrogen atoms are included as spheres of arbitrary size.
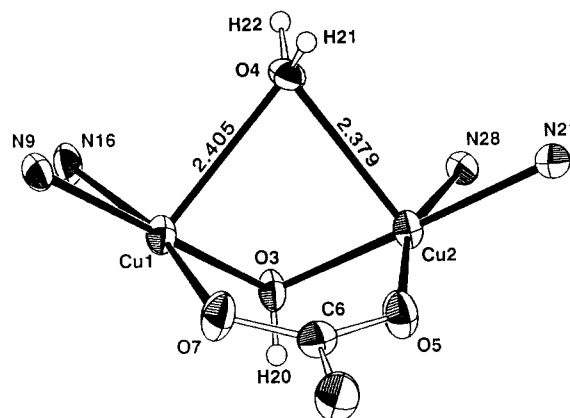
Figure 3. ORTEP representation of the inner coordination sphere of the Cu_2 core for complex **3**.

perchlorate anion; the cations are well separated from each other. The cation represents the first example to our knowledge of a dinuclear copper(II) complex bridged by three carboxylate groups. Two of the acetates are in the familiar bidentate η^1:η^1:μ_2 bridging mode, and the third is in the rare monoatomic bridging mode; a terminal bpy molecule completes five-coordination at each metal atom. The unusual bridging mode for one acetate results in a significant difference between the length of the two carboxylate CO bonds;[7] the C36–O35 distance (1.319 (4) Å) being longer than the C36–O37 distance (1.224 (4) Å). As is sometimes[6,8,18,19a,e,g]

(18) Tolman, W. B.; Bino, A.; Lippard, S. J. *J. Am. Chem. Soc.* **1989**, *111*, 8522.
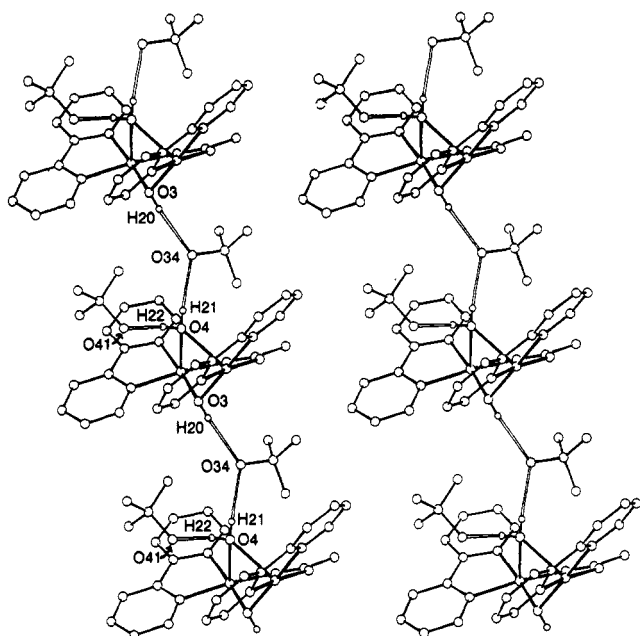
Figure 4. Packing diagram of 3, showing the hydrogen-bonding network and the resulting chains of Cu$_2$ cations. Atoms O34 and O41 belong to two different ClO$_4^-$ anions.

Table II. Fractional Coordinates ($\times 10^4$) and Thermal Parameters ($\times 10$) for Complex 1a

atom	x	y	z	B_{iso}, Å^2
Cu1	6936.7 (3)	3930.4 (2)	6359.6 (5)	12
Cu2	6520.4 (3)	1950.1 (2)	5392.3 (5)	13
N3	5408 (2)	4155 (1)	6591 (3)	12
C4	4300 (3)	3616 (2)	6123 (4)	15
C5	3268 (3)	3811 (2)	6387 (4)	17
C6	3366 (3)	4580 (2)	7188 (4)	16
C7	4484 (3)	5131 (2)	7711 (4)	15
C8	5497 (3)	4904 (2)	7394 (4)	13
C9	6759 (3)	5450 (2)	7865 (4)	13
C10	7070 (3)	6247 (2)	8638 (4)	17
C11	8287 (3)	6714 (2)	8977 (4)	18
C12	9158 (3)	6367 (2)	8545 (4)	19
C13	8791 (3)	5562 (2)	7804 (4)	17
N14	7603 (2)	5105 (1)	7472 (3)	12
N15	5113 (2)	1103 (1)	4280 (3)	13
C16	3888 (3)	1070 (2)	4674 (4)	16
C17	2939 (3)	450 (2)	3887 (4)	16
C18	3254 (3)	-159 (2)	2708 (4)	16
C19	4513 (3)	-128 (2)	2312 (4)	15
C20	5436 (3)	516 (2)	3097 (4)	13
C21	6811 (3)	622 (2)	2772 (4)	13
C22	7295 (3)	52 (2)	1737 (4)	17
C23	8560 (3)	182 (2)	1615 (4)	18
C24	9324 (3)	880 (2)	2493 (4)	19
C25	8805 (3)	1432 (2)	3747 (4)	16
N26	7563 (2)	1309 (1)	3631 (3)	14
O27	8601 (2)	3944 (1)	6222 (3)	17
C28	8792 (3)	3371 (2)	6438 (4)	15
O29	8028 (2)	2606 (1)	6320 (3)	17
C30	10057 (4)	3629 (2)	6870 (6)	25
O31	5541 (2)	3191 (1)	8940 (3)	15
C32	4900 (3)	2429 (2)	9133 (4)	13
O33	5093 (2)	1873 (1)	7901 (3)	16
C34	3738 (4)	2107 (2)	10975 (5)	21
O35	6566 (2)	2985 (1)	4490 (3)	13
C36	7198 (3)	3276 (2)	2782 (4)	18
O37	7833 (2)	4022 (1)	2547 (3)	30
C38	7112 (3)	2644 (2)	1169 (5)	24
Cl39	629 (1)	1503 0(4)	7238 (1)	17
O40	-126 (2)	619 (1)	7056 (3)	24
O41	-268 (2)	1849 (1)	8513 (3)	26
O42	1688 (2)	1702 (1)	7972 (3)	23
O43	1250 (3)	1843 (2)	5416 (3)	36

(but not always[7,19b–d,f,h,20]) observed for monoatomic bridging RCO$_2^-$ groups, there is evidence for an additional weak interaction

Table III. Fractional Coordinates ($\times 10^4$) and Thermal Parameters ($\times 10$) for Complex 3

atom	x	y	z	B_{iso}, Å^2
Cu1	3606 (1)	1617.2 (4)	765 (1)	15
Cu2	1686 (1)	3368.2 (4)	672 (1)	14
O3	2250 (4)	2359 (2)	-769 (5)	16
O4	2246 (4)	2318 (2)	2719 (5)	15
O5	3288 (4)	3657 (2)	1124 (5)	21
C6	4411 (6)	3171 (4)	1351 (7)	19
O7	4701 (4)	2362 (2)	1228 (5)	22
C8	5470 (6)	3576 (4)	1858 (9)	25
N9	4946 (4)	763 (3)	2276 (6)	16
C10	6032 (5)	880 (4)	3271 (8)	18
C11	6916 (6)	243 (4)	4255 (8)	21
C12	6667 (6)	-531 (4)	4229 (9)	22
C13	5559 (6)	-657 (4)	3214 (8)	22
C14	4701 (6)	1 (3)	2237 (7)	15
C15	3490 (5)	-61 (3)	1112 (7)	16
N16	2837 (4)	634 (3)	203 (6)	16
C17	1744 (6)	634 (4)	-891 (8)	20
C18	1234 (6)	-50 (4)	-1137 (8)	23
C19	1876 (6)	-757 (4)	-195 (8)	25
C20	3019 (6)	-768 (4)	920 (8)	22
N21	985 (4)	4414 (3)	2115 (6)	16
C22	1659 (6)	4868 (4)	3216 (7)	18
C23	1097 (6)	5607 (4)	4108 (8)	20
C24	-212 (6)	5887 (4)	3800 (7)	18
C25	-919 (6)	5421 (4)	2668 (8)	18
C26	-310 (5)	4679 (3)	1824 (7)	14
C27	-953 (5)	4127 (3)	586 (7)	15
N28	-171 (4)	3443 (3)	-88 (6)	14
C29	-661 (6)	2911 (4)	-1265 (8)	19
C30	-1959 (6)	3043 (4)	-1780 (9)	24
C31	-2766 (6)	3742 (4)	-1117 (8)	23
C32	-2263 (6)	4290 (4)	81 (8)	22
Cl33	4219 (1)	3128 (1)	6466 (2)	15
O34	3115 (4)	2812 (3)	6248 (5)	21
O35	4047 (5)	3912 (4)	7408 (11)	84
O36	4357 (9)	3240 (8)	4889 (8)	124
O37	5266 (6)	2577 (4)	7376 (12)	100
Cl38	-248 (1)	1835 (1)	4056 (2)	25
O39	607 (4)	2093 (3)	5479 (6)	28
O40	-1179 (6)	2578 (5)	3389 (9)	91
O41	438 (4)	1424 (3)	2737 (6)	27
O42	-796 (9)	1279 (5)	4544 (10)	98

between Cu1 and the nonbridging acetate oxygen atom O37. The Cu1···O37 distance is only 2.716 (2) Å, and the acetate group is clearly tilted toward Cu1, as manifested in the Cu1–O35–C36 angle (108.4 (2)°) being significantly smaller than Cu2–O35–C36 (127.3 (2)°). Also, the Cu1–O35 bridging distance (1.977 (2) Å) is noticeably shorter than the Cu2–O35 distance (2.169 (2) Å). Further, the coordination geometries of the two Cu^{II} atoms are significantly different, and we assign this as also due to the Cu1···O37 interaction. The geometry at Cu1 is best described as distorted square pyramidal with O31 at the apex. As expected, the axial bond is about 0.25 Å longer than bond lengths in the basal plane. Cu1 lies 0.204 Å above the N3, N14, O27, O35 least-squares plane (maximum deviation of 0.319 Å by N14) toward O31. The square-pyramidal description for Cu1 places O37 approximately at the vacant sixth position of the square

(19) (a) Bailey, N. A.; Fenton, D.; Tate, J. R.; Thomas, P. M. *J. Chem. Soc., Dalton Trans.* **1985**, 1471. (b) Chiari, B.; Hatfield, W. E.; Piovesana, O.; Tarantelli, T.; Haar, L. W. T.; Zanazzi, P. F. *Inorg. Chem.* **1983**, 22, 1468. (c) Chiari, B.; Piovesana, O.; Tarantelli, T.; Zanazzi, P. F. *Inorg. Chem.* **1985**, 24, 4615. (d) Boukari, Y.; Busnot, A.; Busnot, F.; Leclaire, A.; Bernard, M. A. *Acta Crystallogr., Sect. B* **1982**, B38, 2458. (e) Hämäläinen, R.; Ahlgrén, M.; Turpeinen, U. *Acta Crystallogr., Sect. B* **1982**, 38, 1577. (f) Chiari, B.; Helms, J. H.; Piovesana, O.; Tarantelli, T.; Zanazzi, P. F. *Inorg. Chem.* **1986**, 25, 870. (g) Chiari, B.; Helms, J. H.; Piovesana, O.; Tarantelli, T.; Zanazzi, P. F. *Inorg. Chem.* **1986**, 25, 2408. (h) Chiari, B.; Piovesana, O.; Tarantelli, T.; Zanazzi, P. F. *Inorg. Chem.* **1988**, 27, 3246.
(20) (a) Yawney, D. B. W.; Moreland, J. A.; Doedens, R. J. *J. Am. Chem. Soc.* **1973**, 95, 1164. (b) Brown, J. N.; Trefonas, L. M. *Inorg. Chem.* **1973**, 12, 1730. (c) Osterberg, R.; Sjöberg, B.; Söderquist, R. *J. Chem. Soc., Chem. Commun.* **1972**, 983.

Table IV. Selected Bond Distances (Å) and Angles (deg) for **1a**

(a) Bonds

Cu1···Cu2	3.392 (1)	Cu1···O37	2.716 (2)
Cu1–O27	1.939 (2)	Cu2–O29	1.930 (2)
Cu1–O31	2.238 (2)	Cu2–O33	1.974 (2)
Cu1–O35	1.977 (2)	Cu2–O35	2.169 (2)
Cu1–N3	2.001 (2)	Cu2–N15	1.992 (2)
Cu1–N14	2.019 (2)	Cu2–N26	2.033 (2)
C36–O35	1.319 (4)	C32–O33	1.270 (3)
C36–O37	1.224 (4)	C28–O27	1.255 (3)
C32–O31	1.245 (3)	C28–O29	1.259 (4)

(b) Angles

O27–Cu1–O31	97.4 (1)	Cu1–O35–Cu2	109.8 (1)
O27–Cu1–O35	93.6 (1)	O29–Cu2–O33	94.9 (1)
O31–Cu1–O35	96.5 (1)	O29–Cu2–O35	96.0 (1)
O27–Cu1–N3	168.8 (1)	O29–Cu2–N15	168.3 (1)
O27–Cu1–N14	88.3 (1)	O29–Cu2–N26	88.6 (1)
O31–Cu1–N3	87.6 (1)	O33–Cu2–O35	96.7 (1)
O31–Cu1–N14	102.4 (1)	O33–Cu2–N15	90.6 (1)
O31–Cu1–O37	149.4 (2)	O33–Cu2–N26	140.1 (1)
O35–Cu1–N3	95.9 (1)	O35–Cu2–N15	93.7 (1)
O35–Cu1–N14	160.6 (1)	O35–Cu2–N26	122.6 (1)
N3–Cu1–N14	80.8 (1)	N15–Cu2–N26	80.6 (1)
Cu1–O35–C36	108.4 (2)	Cu2–O35–C36	127.3 (2)
Cu1–O31–C32	131.4 (2)	Cu2–O33–C32	131.4 (2)
Cu1–O27–C28	129.7 (2)	Cu2–O29–C28	134.2 (2)

pyramid (O31–Cu1–O37 = 149.4 (2)°). In contrast, Cu2 is better described as a distorted trigonal bipyramid (O29–Cu2–N15 = 168.3 (1)°), with Cu2 lying 0.093 Å out of the equatorial plane toward O29. An alternative description for Cu2 is severely distorted square pyramidal with O35 in the apex; this is less preferred. The indicated geometries at Cu1 and Cu2 are further supported by a detailed analysis of the Cu coordination polyhedra using the method of Muetterties and Guggenberger.[21] The Cu–N distances, and their slight variation as a function of axial vs equatorial location at Cu2, are typical of Cu^{II}/bpy complexes.[22]

The monoatomic bridging mode for acetate is relatively uncommon; we are aware of eleven previous examples in copper(II) acetate chemistry[6–8,19] and three with other carboxylato ligands.[20] In Table V are compared some structural parameters for Cu^{II} complexes with monoatomic acetate bridges. Complex **1a** has an unremarkable Cu···Cu separation but the largest Cu–O–Cu angle (109.8 (1)°) yet observed. Note that Cu···Cu separations are much larger than those seen in the classic "$Cu_2(O_2CR)_4 \cdot L_2$" structures where the four bidentate bridging carboxylates allow a much closer approach of the metals (~2.6–2.7 Å).[2b] Table V also shows that monoatomic bridging acetate oxygens usually occupy an equatorial/basal position for one metal and an axial/apical position for the other metal, leading to large differences in Cu–O bond lengths (0.5–0.7 Å). This is not the case in **1a**, and the Cu–O distances are less different as a result.

The structure of the cation of complex **3** again consists of a triply bridged pair of five-coordinate copper atoms, but only one of the bridging ligands is an acetate group, the others being an OH^- ion and a H_2O molecule. The acetate group is in the familiar bidentate $\eta^1:\eta^1:\mu_2$-bridging mode; a terminal bpy molecule completes five-coordination at each metal atom. The Cu···Cu separation in **3** is noticeably shorter than in **1a** (3.035 (2) vs 3.392 (1) Å) presumably due to the greater number of monoatomic bridges. The metal coordination geometries are best described as square pyramidal with the water oxygen O4 occupying the apical positions for both metals. The inner coordination sphere of the Cu atoms is shown in Figure 3. As expected, the apical Cu–O4 distances are noticeably longer than basal bond distances. Cu1 is only 0.092 Å out of the O3, O7, N9, N16 plane (maximum deviation by N9 of 0.078 Å), and Cu2 is only 0.137 Å out of the O3, O5, N21, N28 plane (maximum deviation by N21 of 0.140

Å); as a result, the Cu centers could be acceptably considered as square planar, each with a weak axial bond to the water molecule (O4); this viewpoint is particularly emphasized by Figure 3. The dihedral angle between the two CuN_2O_2 planes is 61.9°.

The cations of **3** form infinite chains as a result of H-bonding interactions with the ClO_4^- anions (Table VII). Oxygen atom O34 of one ClO_4^- H-bonds to both OH^- hydrogen H20 of one cation and H_2O hydrogen H21 of an adjacent cation; this serves to form the infinite chain as shown in Figure 4. The other ClO_4^- (O41) is H-bonded to the second H_2O hydrogen H22 but does not bridge to another cation. The H-bonding network shown in Figure 4 is of particular importance to the magnetic properties of **3** (vide infra).

Two other Cu_2 complexes should be mentioned at this point: (i) $[Cu_2(OH)(H_2O)L(ClO_4)_2]^+$ (L = a binucleating macrocyclic ligand) is the only other example[23] of a dinuclear Cu^{II} complex bridged by both OH^- and H_2O. It, too, has long $Cu–O(H_2O)$ linkages (2.519 (12) Å) and an acute $Cu–O(H_2)–Cu$ angle of 77.3 (4)° similar to that in **3** (78.7 (1)°). (ii) $[Cu_2(OH)(MeOH)(OAc)(L-L)]^{2+}$ (L-L = a binucleating tetradentate ligand) comes closest to reproducing the $Cu_2(OH)(H_2O)(OAc)$ core of **3**; it has a bridging MeOH instead of the bridging H_2O. The Cu–O(MeOH) distances are, however, somewhat longer (2.59 (1) Å), and the authors prefer to describe it as a MeOH inclusion compound rather than MeOH-bridged.[10a]

IR and UV/Vis Spectroscopy. Complexes **1a**, **1b**, and **4** possess very similar solid-state electronic spectra, supporting similar structures for their cations. Both exhibit acetate-to-copper LMCT transitions[24] in the 383–353-nm range and d–d transitions at lower energies. The large number of d–d maxima probably reflect the two different metal geometries within the complex. The band at 355 nm in **3** is assigned to hydroxide or acetate LMCT.[24] The d–d spectrum of **3** is characteristic of its five-coordinate square-pyramidal structure.[24,25] The spectrum exhibits maxima at 590, 625, and 1115 nm, which are assigned to $B_1 \rightarrow E$, $B_1 \rightarrow B_2$, and $B_1 \rightarrow A_1$ transitions, respectively, in C_{4v} symmetry; however, the actual lower symmetry will cause splitting of the tetragonal ^2E state and result in four possible transitions, two of which are probably unresolved.[25] The d–d spectra of **1a** in MeCN and CH_2Cl_2 consist of a very broad, featureless band at 686 and 706 nm, respectively; this slight difference in wavelength reflects different degrees of cation–solvent interactions, and it is possible that MeCN may be bound as a sixth ligand.

In the IR spectra, complex **3** exhibits a medium-intensity band at 3535 cm^{-1} due to the bridging O–H;[26] its broadness and relatively low frequency are both indicative of hydrogen bonding. In addition, **3** exhibits a broad medium $\nu(OH)_{H_2O}$ band at 3410 and a $\delta(HOH)$ band at 1611 cm^{-1}.[26] The ClO_4^- mode at ~1100 cm^{-1} in **3** is somewhat broadened, indicating the involvement of this anion in hydrogen bonding. The $\nu_{as}(COO)$ and $\nu_s(COO)$ bands of **3** are at 1555 and 1448 cm^{-1}, respectively; the difference (107 cm^{-1}) is less than that for NaO_2CMe (164 cm^{-1}), as expected for this mode of carboxylate ligation.[26,27] Owing to the presence of two different types of acetate bridges in **1a**, two $\nu_{as}(COO)$ (1638, 1601 cm^{-1}) and two $\nu_s(COO)$ (1448, 1371 cm^{-1}) bands are observed. The bands at 1638 and 1371 cm^{-1} are assigned to the stretching modes of the monoatomic acetate bridge, and those at 1601 and 1448 cm^{-1} to the triatomic acetate bridges.[26,27] Owing to the asymmetric bonding mode of the monoatomic carboxylate group, a large splitting ($\Delta = 267$ cm^{-1}) of the –COO stretching frequencies is observed. A quite similar spectral pattern for the carboxylate stretching frequencies is observed for complexes **1b** and **4**, suggesting that they have an analogous structure with both

(21) Muetterties, E. L.; Guggenberger, L. J. *J. Am. Chem. Soc.* **1974**, *96*, 1748.

(22) Haddad, M. S.; Wilson, S. R.; Hodgson, D. J.; Hendrickson, D. N. *J. Am. Chem. Soc.* **1981**, *103*, 384 and references therein.

(23) Drew, M. G. B.; Nelson, J.; Esho, F.; McKee, V.; Nelson, S. M. *J. Chem. Soc., Dalton Trans.* **1982**, 1837.

(24) Lever, A. B. P. *Inorganic Electronic Spectroscopy*, 2nd ed.; Elsevier: Amsterdam, 1984; pp 356, 553–572, 636–638.

(25) Reinen, D.; Friebel, C. *Inorg. Chem.* **1984**, *23*, 791.

(26) Nakamoto, K. *Infrared and Raman Spectra of Inorganic and Coordination Compounds*, 4th ed.; Wiley: New York, 1986; pp 147–150, 227–233, 251–253.

(27) Deacon, G. B.; Phillips, R. J. *Coord. Chem. Rev.* **1980**, *33*, 227.

Table V. Relevant Structural Parameters for Monoatomic Acetate-Bridged Copper(II) Complexes

complex	Cu–O, Å		Cu···Cu, Å	Cu–O–Cu, deg	ref
	equatorial/basal	axial/apical			
Cu$_2$(*i*-PrOHSal)$_2$(O$_2$CMe)$_2$^{a}	1.952	2.446	3.445	102.6	6
	1.952	2.651		95.7	
Cu$_2$(O$_2$CMe)$_4$L$_4$^{b,c}	1.986	2.424	*d*	102.45	19d
[Cu$_2$L′(O$_2$CMe)$_2$]$_n$^{e}	1.952	2.495	3.383	98.3	19b
Cu$_2$(AE)$_2$(O$_2$CMe)$_2$^{f}	1.955	2.490	3.305	95.3	7
Cu$_2$L″(O$_2$CMe)$_2$^{g}	1.971	2.486	3.507	101.3	19a
	1.981	2.540		103.0	
Cu$_2$(Pypep)$_2$(O$_2$CMe)$_2$^{h}	1.987	2.497	3.542	*d*	8
Cu$_3$L‴$_2$(O$_2$CMe)$_4$^{i,j}	2.000		3.319	98.2	19c
	2.377				
Cu$_2$A$_2$(O$_2$CMe)$_2$^{k}	1.978	2.512	3.379	96.9	19e
[Cu$_2$A′$_2$(O$_2$CMe)$_2$(H$_2$O)$_2$]$_n$^{l}	1.960	2.498	3.384	98.1	19f
Cu$_2$A″$_2$(O$_2$CMe)$_2$^{m}	1.976	2.577	3.409	96.1	19g
Cu$_2$A‴$_2$(O$_2$CMe)$_2$^{n}	2.003	2.665	3.506	96.3	19g
[Cu$_4$A⁗$_2$(O$_2$CMe)$_6$(EtOH)$_2$]$_n$^{o,p}	1.980	2.570	3.475	98.2	19h
[Cu$_2$(O$_2$CMe)$_3$(bpy)$_2$]$^+$	1.977		3.392	109.8	*q*
	2.169				

^{a} *i*-PrOHSal = *N*-(1,1-dimethyl-2-hydroxyethyl)salicylaldiminato(1−). ^{b} L = 1-methylimidazole. ^{c} Only two of the acetate groups are bridging. ^{d} Not reported. ^{e} L′ = dianion of *N*,*N*′-bis(2-((o-hydroxybenzhydrylidene)amino)ethyl)-1,2-ethanediamine. ^{f} AE = the anion of 7-amino-4-methyl-5-aza-3-hepten-2-one. ^{g} L″ = 6-amino-1-(2′-hydroxylphenyl)-3-methyl-4-azahepta-2-en-1-onato(1−). ^{h} Pypep = monoanion of *N*-(2-(4-imidazolyl)ethyl]pyridine-2-carboxamide. ^{i} L‴ = monoanion of *N*-methyl-*N*′-(4-methoxysalicylidene)-1,3-propanediamine. ^{j} There are two types of acetate bridges between each pair of adjacent copper ions in the linear trimer, a Cu–O–C–O–Cu bridge and a monoatomic bridge. ^{k} A = anion of *N*-methyl-*N*′-salicylidene-1,3-propanediamine. ^{l} A′ = anion of *N*-methyl-*N*′-(5-methoxysalicylidene)-1,3-propanediamine. ^{m} A″ = anion of *N*-methyl-*N*′-(5-nitrosalicylidene)-1,3-propanediamine. ^{n} A‴ = anion of *N*-methyl-*N*′-(5-bromosalicylidene)-1,3-propanediamine. ^{o} A⁗ = anion of *N*-methyl-*N*′-(4,6-dimethoxysalicylidene)-1,3-propanediamine. ^{p} Only two of the acetate groups are monoatomic bridging. ^{q} This work.

Table VI. Selected Bond Distances (Å) and Angles (deg) for **3**.

(a) Bonds

Cu1···Cu2	3.035 (2)		
Cu1–O3	1.927 (4)	Cu2–O3	1.930 (4)
Cu1–O4	2.405 (4)	Cu2–O4	2.379 (4)
Cu1–O7	1.931 (4)	Cu2–O5	1.944 (4)
Cu1–N9	2.006 (5)	Cu2–N21	2.010 (5)
Cu1–N16	2.008 (5)	Cu2–N28	2.009 (4)
C6–O7	1.267 (7)	C6–O5	1.264 (7)

(b) Angles

Cu1–O3–Cu2	103.8 (2)	O3–Cu2–O4	80.9 (2)
Cu1–O4–Cu2	78.7 (1)	O3–Cu2–O5	94.2 (2)
O3–Cu1–O4	80.3 (1)	O3–Cu2–N21	176.3 (2)
O3–Cu1–O7	95.2 (2)	O3–Cu2–N28	95.4 (2)
O3–Cu1–N9	175.0 (2)	O4–Cu2–O5	98.7 (2)
O3–Cu1–N16	93.9 (2)	O4–Cu2–N21	99.4 (2)
O4–Cu1–O7	98.2 (2)	O4–Cu2–N28	98.2 (2)
O4–Cu1–N9	100.5 (2)	O5–Cu2–N21	89.4 (2)
O4–Cu1–N16	92.9 (2)	O5–Cu2–N28	161.6 (2)
O7–Cu1–N9	89.6 (2)	N21–Cu2–N28	80.9 (2)
O7–Cu1–N16	166.7 (2)	Cu2–O5–C6	129.6 (4)
N9–Cu1–N16	81.2 (2)	Cu1–O7–C6	129.4 (4)

Table VII. Hydrogen-bonding Distances (Å) and Angles (deg) in **3**

O4···O34	2.87 (1)	O4···O41	2.85 (1)
H21···O34	2.16 (9)	H22···O41	2.02 (10)
O4–H21–O34	172 (9)	O4–H22–O41	169 (9)
O3···O34	3.05 (1)	O3–H20–O34	175 (9)
H20···O34	2.29 (10)		

monoatomic and triatomic carboxylate bridges.

Electrochemical Studies. Complexes **1a** and **3** were studied by using the cyclic voltammetry technique. Complex **3** displayed only broad, ill-defined and grossly irreversible features; complex **1a**, however, displayed some interesting behavior. The CV (cyclic voltammogram) of **1a** is shown in Figure 5. The complete scan (bottom trace) showed two cathodic processes of comparable peak currents at E_p values of −0.81 and −1.80 V, and a large anodic feature at −0.57 V on the reverse scan characteristic of an electrochemically active species adsorbed on the electrode. We suspected this to be Cu metal and confirmed this in a subsequent scan (with a polished electrode) by holding the potential at −2.11 V for 3 min and clearly observing a film of Cu metal on examination of the electrode surface. This suggested that the cathodic
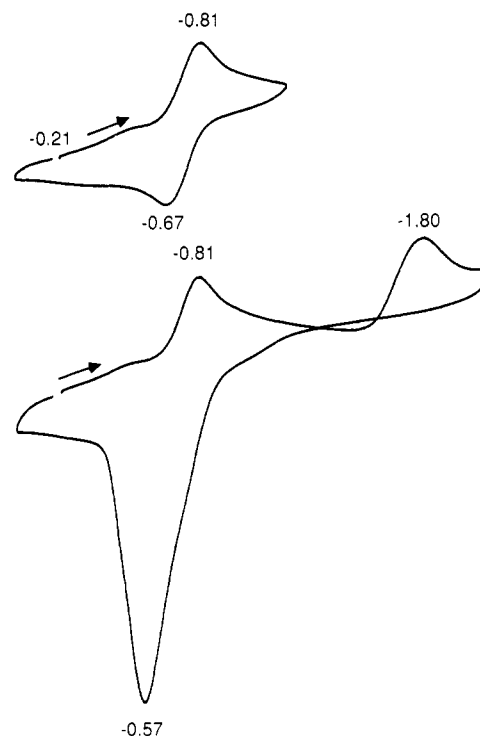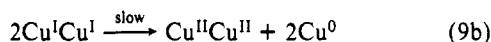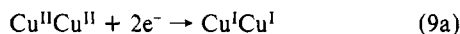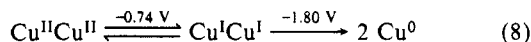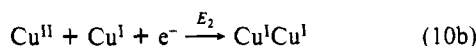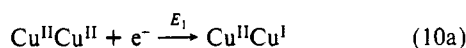

Figure 5. Cyclic voltammograms of complex **1a** in MeCN (1 mM) in the ranges −0.01 to −1.21 V (top) and −0.01 to −2.11 V (bottom). Potentials are quoted vs ferrocene (+0.51 V vs SCE under the same conditions).

features were both two-electron reduction waves, and peak currents were certainly larger than expected for a one-electron process. Reversal of the potential at −1.21 V revealed the first process to be quasi-reversible ($E_{1/2}$ = −0.74 V, ΔE_p = 0.14 V, $i_p^a/i_p^c \approx 1$). We sought to confirm the two-electron ($n = 2$) nature of the first wave by controlled-potential coulometry at −1.10 V but were surprised to obtain a value of $n = 3.97$ (i.e., four-electron transfer). Even a (much slower) electrolysis performed at −0.8 V gave a value >2 (in fact, $n \approx 3.0$). These observations strongly suggest that the two-electron reduction at −0.74 V is followed by a disproportionation that is slow on the CV time scale, as summarized in eqs 8 and 9. In the CV, the behavior in eq 8 is observed,

$$Cu^{II}Cu^{II} \xrightleftharpoons{-0.74 \text{ V}} Cu^{I}Cu^{I} \xrightarrow{-1.80 \text{ V}} 2 Cu^0 \qquad (8)$$

$$Cu^{II}Cu^{II} + 2e^- \rightarrow Cu^{I}Cu^{I} \qquad (9a)$$

$$2Cu^{I}Cu^{I} \xrightarrow{slow} Cu^{II}Cu^{II} + 2Cu^0 \qquad (9b)$$

whereas eqs 9a and 9b summarize the coulometry behavior. Clearly, the latter will give $n = 4$ because each Cu^{II}_2 molecule is overall reduced by four electrons and converted to 2 Cu^0, the disproportionation (eq 9b) continuously regenerating more $Cu^{II}Cu^{II}$ for reduction in eq 9a. The scheme outlined in eq 9 is supported by the following studies and results in the concentration range 0.5–2.5 mM: the peak potentials shift cathodically with increasing concentration; $i_p^c/v^{1/2}$ decreases markedly with increasing scan rate (v); i_p^a/i_p^c increases with increasing v and decreases with increasing concentration.[28a] These are all diagnostic criteria for a disproportionation following electron transfer.[29a]

The observation of only a single, two-electron wave at −0.74 V suggests the difference between the two potentials (E_1 and E_2) of the two one-electron couples to be <180 mV (eqs 10a and 10b).
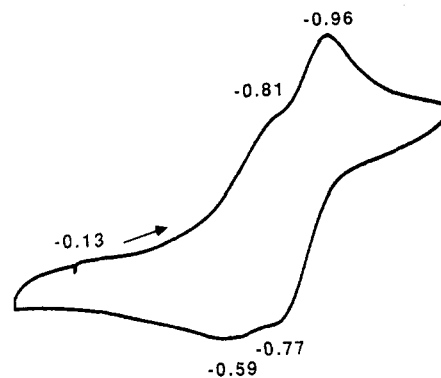
$$Cu^{II}Cu^{II} + e^- \xrightarrow{E_1} Cu^{II}Cu^{I} \qquad (10a)$$

$$Cu^{II} + Cu^{I} + e^- \xrightarrow{E_2} Cu^{I}Cu^{I} \qquad (10b)$$

With the ferrocene response in MeCN as a reference ($\Delta E_p \approx 0.09$V), the large peak separation ($\Delta E_p = 0.14$ V) argues for the second reduction being more difficult than the first; i.e., E_2 is more cathodic than E_1. The opposite case should give ΔE_p values smaller than those for a one-electron process.[29a] The quasi-reversible nature of the couple makes a more quantitative determination of $E_2 - E_1$ unreliable, and it has not been attempted. Interestingly, in CH_2Cl_2 the two one-electron processes (eqs 10a and 10b) are resolved (Figure 6), providing direct evidence for the two-electron process; the obtained parameters are $E_1 = -0.70$ V, $\Delta E_p^1 \approx 0.2$ V, $E_2 = -0.86$ V, and $\Delta E_p^2 = 0.19$ V.[28b] The low solubility of **1a** in CH_2Cl_2 prevented extensive investigation in this solvent. Complex **4** in MeCN gave CV features identical with those of **1a**, with parameters $E_{1/2} = -0.72$ V and $\Delta E_p = 0.14$ V.

Finally, we comment on the small feature at $\sim$−0.5 V preceding the first cathodic wave for **1a** (Figure 5) and its barely discernible partner on the reverse scan. We originally suspected it to be due to an impurity, but recrystallized samples displayed identical behavior. We then suspected a monomer/dimer equilibrium, facilitated by the donor properties of MeCN, with the small feature due to a small amount of monomer; however, complex **1** rigorously obeys Beer's law in MeCN (0.5–10 mM). It is also observed in the CV of complex **4** (same position relative to the main wave). Further, it is evident in poorly coordinating CH_2Cl_2 (Figure 6); the forward feature is noticeable as a distortion of the base of the first cathodic wave, and the reverse scan barely reveals it. It is, however, absent in DMF. We believe the most likely explanation is that the feature is due to adsorption effects. Since it is anodic to the main wave ("prewave"), this is consistent with adsorption of *product* onto the electrode surface.[29b]

Magnetic Susceptibility Studies. Variable-temperature magnetic susceptibility data were collected on powdered samples of complexes **1a** and **3** in the temperature range 5.0–300.0 K. The data were least-squares fit to the Bleaney–Bowers equation[30] based on the Hamiltonian $H = -2JS_1 \cdot S_2$, replacing T with $(T - \Theta)$, where Θ is the Weiss constant.

For complex **1a**, the effective magnetic moment, μ_{eff}, per Cu_2 decreases gradually from 2.96 μ_B at 295.0 K to a minimum of
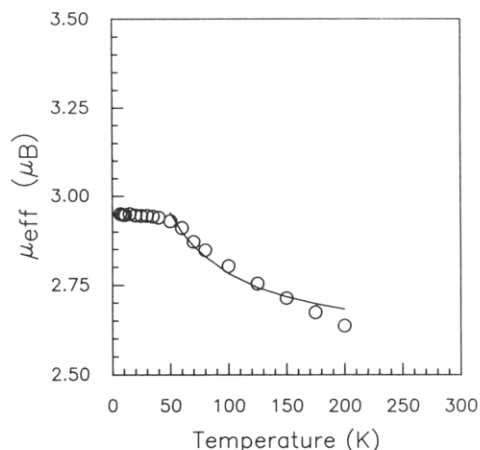
(28) (a) Only at low scan rates, presumably due to the slow rate of disproportionation. (b) Half-wave potentials were obtained from differential-pulse voltammetry.

(29) (a) Brown, E. E.; Sandifer, J. R. In *Physical Methods of Chemistry*, 2nd ed.; Rossiter, B. W., Hamilton, J. F., Eds.; Wiley: New York, 1986; Vol. 2, pp 273–429. (b) Bard, A. J.; Faulkner, L. R. *Electrochemical Methods*; Fundamentals *and Applications*; Wiley: New York, 1980.

(30) Bleaney, B.; Bowers, K. D. *Proc. R. Soc. London, A* **1952**, *214*, 451.

Figure 6. Cyclic voltammogram of complex **1a** in CH_2Cl_2 (0.8 mM) in the range +0.07 to −1.33 V. Potentials are quoted vs ferrocene (+0.53 V vs SCE under the same conditions).
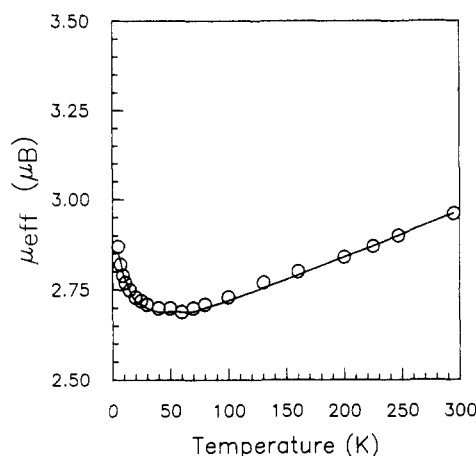
Figure 7. Plot of the effective magnetic moment per dinuclear complex, μ_{eff}/Cu_2, vs temperature for a polycrystalline sample of complex **1a**. The solid line results from a least-squares fit of the data to the Bleaney–Bowers equation. See the text for fitting parameters.

2.69 μ_B at 60.0 K and then rises to 2.87 μ_B at 5.0 K (Figure 7). The behavior is clearly indicative of intramolecular ferromagnetic exchange interactions. A satisfactory fit of the data was obtained with $J = +3.6$ cm^{-1}, $g = 2.1$, and $\theta = 0.20$ K (solid line in Figure 7).

Ferromagnetic exchange interactions are also present in complex **3**. The effective magnetic moment per Cu_2 rises gradually from 2.64 μ_B at 200 K to 2.93 μ_B at 50.0 K and then is relatively constant with a value of 2.95 μ_B at 5.0 K (Figure 8). In attempts to fit the data to the Bleaney–Bowers equation, it became evident that the experimental data in the 5.0–50.0 K region could not be accommodated by this equation. After consideration of possible reasons for the poor quality of the fit in this low-temperature region, it was concluded that the most likely explanation was weak *inter*molecular *anti*ferromagnetic interactions. The cations of **3** are hydrogen bonded to the ClO_4^- ions, and one of the ClO_4^- anions serves to bridge neighboring cations to give infinite chains, as mentioned earlier and shown in Figure 4. Intermolecular antiferromagnetic interactions mediated by hydrogen-bonding networks have precedence in Cu^{II} chemistry.[31] The effects of these additional and weak exchange interactions would be particularly important in the low-temperature region, and we believe this to be the cause of the inability of the theoretical model to account for the experimental data. The present data are not discriminating enough to warrant the use of a more sophisticated model involving chains of interacting magnetic centers. We used only the 50.0–200 K data to obtain an estimate of J. Shown as a solid line in Figure

(31) (a) Eduok, E. E.; O'Connor, C. J. *Inorg. Chim. Acta* **1984**, *88*, 229. (b) Bertrand, J. A.; Fujita, E.; van Der Veer, D. G. *Inorg. Chem.* **1980**, *19*, 2022 and references therein. (c) Laskowski, E. J.; Duggan, D. M.; Hendrickson, D. N. *Inorg. Chem.* **1975**, *14*, 2449.

Figure 8. Plot of the effective magnetic moment per dinuclear complex, μ_{eff}/Cu_2, vs temperature for a polycrystalline sample of complex **3**. The solid line results from a least-squares fit of the data to the Bleaney–Bowers equation. See the text for fitting parameters.

8 is a fit to the 50–200 K data, which is characterized by $J = +19.3$ cm^{-1}, $g = 2.1$, and $\Theta = 4.5$ K.

Although dinuclear Cu^{II} complexes usually display antiferromagnetic exchange interactions,[2] ferromagnetic systems are by no means rare. Complexes **1a** and **3** are two new members of this latter class, and the magnitudes of their exchange parameter J fall within the typical range observed for previous examples.[2c,6,10a,c,d,11a,32] Since the observed J values are composed of ferromagnetic and antiferromagnetic contributions,[33] and these are in turn influenced by a variety of structural and electronic factors, it is difficult to give a definitive explanation for the net ferromagnetism observed, although some pertinent observations and partial rationalization will be attempted. The two Cu^{II} coordination geometries in **1a** will lead to different electronic structures. For square-pyramidal Cu1, the magnetic orbital is $d_{x^2-y^2}$ with lobes directed toward O35 and O27. For trigonal-bipyramidal Cu2, however, the magnetic orbital is d_{z^2} with unpaired spin density primarily along the N15–Cu2–O29 axis. In addition, the differing geometries mean that the magnetic orbitals will be of different energies. These facts, together with the relatively long Cu2–O35 bond (2.169 (2) Å), suggest this σ pathway provides at best only a weak antiferromagnetic contribution and may, therefore, with perhaps other factors, be a major cause of the observed ferromagnetic exchange interaction. It was noted earlier that the geometry at Cu2 could be described as distorted square pyramidal with O35 at the apex. Under this description, the Cu2 magnetic orbital is $d_{x^2-y^2}$, resulting in a σ/δ orthogonality of the magnetic orbitals for the (presumably dominating) Cu1–O35–Cu2 pathway and rationalizing the observed ferromagnetic interaction.

For complex **3**, both Cu centers are square pyramidal with the H$_2$O (O4) at the apex. The magnetic orbital is $d_{x^2-y^2}$ for both metals, with lobes directed toward the two bridging ligands OH$^-$ and MeCO$_2^-$. The exchange interactions within bis-[2c,34] and mono(μ-hydroxo)[11a,22,35] Cu$^{II}_2$ systems have been well investigated, and the magnitude and sign of the interaction have been found to be sensitive to a number of factors including the Cu–O–Cu angle and the dihedral angle between the two Cu-based planes. The bridging angle in **3** is 103.8 (2)°, a relatively small value that may be contributing to the observed ferromagnetism; larger angles (~120°) generally result in antiferromagnetic interactions.
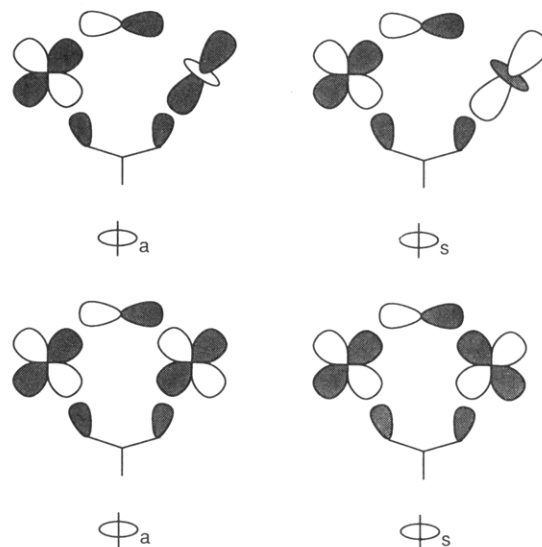
Figure 9. Overlap of the antisymmetric (ϕ_a) and symmetric (ϕ_s) combinations of the magnetic orbitals of **1a** (top) and **3** (bottom) with the bridging ligands, showing the "noncomplementary" nature of the overlap.

An alternative and perhaps firmer rationalization for the ferromagnetism in complexes **1a** and **3** is provided by reference to the work of Hoffmann,[36] Nishida,[10b,37] and Reed.[38] Hoffmann[36] has concluded that the magnitude of antiferromagnetic exchange interactions in dinuclear systems is proportional to the energy separation between the symmetric (ϕ_s) and antisymmetric (ϕ_a) combinations of the magnetic orbitals, no matter which orbital is lower in energy. The magnetic orbitals are antibonding with respect to interactions with filled orbitals on bridging ligands, and the energy separation between ϕ_a and ϕ_s will depend on the nature of the overlap between these orbitals and those on the bridging ligands. Specifically for the combination of one RCO$_2^-$ and one RO$^-$ (R = alkyl, H), Reed[38] and Nishida[37] have shown that the interactions of these ligands with $d_{x^2-y^2}/d_{x^2-y^2}$ or d_{z^2}/d_{z^2} magnetic orbitals are "noncomplementary"; i.e, each bridging ligand will destabilize a different member of the ϕ_a/ϕ_s pair and have no net overlap with the other member. If the extents of destabilization of ϕ_a and ϕ_s are comparable, these two orbitals may have essentially identical energies and ferromagnetic coupling will result. The overlaps in **1a** ($d_{x^2-y^2}/d_{z^2}$) and **3** ($d_{x^2-y^2}/d_{x^2-y^2}$) are shown in Figure 9, and it can clearly be seen that for neither possibility (ϕ_a or ϕ_s) do *both* bridging ligands have antibonding overlaps; each orbital is destabilized by only one bridging ligand. We suggest that the resulting destabilization of the ϕ_a and ϕ_s combinations is essentially equivalent in magnitude, leading to the observed ferromagnetic coupling. It is interesting to note that a few Cu$^{II}_2$ systems bridged by RCO$_2^-$ and one RO$^-$ ligand (R = H, alkyl, MeCO) are now known to be weakly antiferromagnetic or ferromagnetic,[37,38] and it is possible that noncomplementarity of ligand orbitals and nearly equivalent destabilization of ϕ_a and ϕ_s are the common explanation.

Concluding Comments. The use of chelating bpy enforces a rearrangement of the Cu$_2$(O$_2$CMe)$_4$ quadruply bridged core and yields two members of a what promises to be a new family of Cu/RCO$_2^-$/bpy complexes. Both products have bridging units not observed previously in Cu$_2$ chemistry and provide new examples of ferromagnetically coupled systems. Work in progress at the time of writing is providing additional members of this family with different structures and bridging units; this work will be described in a subsequent report.

(32) Mallah, T.; Kahn, O.; Gouteron, J.; Jeannin, S.; Jeannin, Y.; O'Connor, C. J. *Inorg. Chem.* **1987**, *26*, 1375.

(33) (a) Kahn, O. *Inorg. Chim. Acta* **1982**, *62*, 3. (b) Kahn, O.; Charlot, M. F. *Nouv. J. Chim.* **1980**, *4*, 567.

(34) Charlot, M. F.; Jeannin, S.; Jeannin, Y.; Kahn, O.; Lucrece-Abaul, J. *Inorg. Chem.* **1979**, *18*, 1675.

(35) Thompson, L. K.; Lee, F. L.; Gabe, E. J. *Inorg. Chem.* **1988**, *27*, 39 and references cited therein.

(36) Hay, P. J.; Thibeault, J. C.; Hoffmann, R. *J. Am. Chem. Soc.* **1975**, *97*, 4884.

(37) Nishida, Y.; Taueuchi, M.; Takahashi, K.; Kida, S. *Chem. Lett.* **1985**, 631.

(38) McKee, V.; Zvagulis, M.; Reed, C. A. *Inorg. Chem.* **1985**, *24*, 2914.

assistance with the coulometry, and S. Wang for help with figure preparation.

Supplementary Material Available: Complete listings of crystallographic data, hydrogen coordinates and isotropic parameters, anisotropic thermal parameters, and bond distances and angles (19 pages); tables of calculated and observed structure factors (17 pages). Ordering information is given on any current masthead page. Complete MSC structure reports (Nos. 88087 and 88124 for **1a** and **3**, respectively) are available on request from the Indiana University Chemistry Library.

Contribution from the Department of Chemistry, University of Illinois at Urbana-Champaign, 505 South Mathews Avenue, Urbana, Illinois 61801

High-Resolution Aluminum-27 Solid-State Magic-Angle Sample-Spinning Nuclear Magnetic Resonance Spectroscopic Study of AlCl₃–Tetrahydrofuran Complexes†

Oc Hee Han‡ and Eric Oldfield*

We have obtained ^{27}Al solid-state nuclear magnetic resonance (NMR) spectra of several AlCl₃–THF complexes, using "magic-angle" sample-spinning (MASS) NMR at high field. Our results suggest that the isotropic chemical shifts (δ_i) occur in relatively well defined regions for 4-, 5-, and 6-coordinate species (AlCl₄⁻, ~103 ppm; AlCl₃·THF, ~99 ppm; *trans*-AlCl₃·2THF, ~60 ppm; *trans*-[AlCl₂(THF)₄]⁺, ~14 ppm), as found previously with aluminum oxo compounds. We also find that theoretically calculated average nuclear quadrupole coupling constants (e^2qQ/h) (*trans*-[AlCl₂(THF)₄]⁺, ~6.3 MHz; *trans*-AlCl₃·2THF, ~4.6 MHz; AlCl₃·THF, ~3.0 MHz; AlCl₄⁻, 0 MHz) are in good accord with experimentally determined nuclear quadrupole coupling constants, determined from computer simulations of the MASS NMR spectra (*trans*-[AlCl₂(THF)₄]⁺, 6.4 MHz; *trans*-AlCl₃·2THF, 4.9 MHz; AlCl₃·THF, 4.7 MHz; AlCl₄⁻, 0.3 MHz). Both ^{27}Al δ_i and e^2qQ/h determinations appear to be useful as probes of structure in these systems, and thus offer a facile means of monitoring various solid-state reactions.

Introduction

The structure of the various complexes of aluminum chloride with organic Lewis bases has been the subject of investigation for many years, due at least in part to the fact that some aluminum complexes participate in catalytic reactions. There has been considerable interest in the AlCl₃–tetrahydrofuran (THF) system,[1-4] which we found of interest since it could relate to our studies of AlCl₃–graphite intercalation compounds—where questions as to the nature of the AlCl$_n$ complexes remain.[5] The AlCl₃–THF system has been extensively studied, since it can yield several kinds of complex. In the liquid state, AlCl₃·THF, *cis*- and *trans*-AlCl₃·2THF, AlCl₄⁻, and [AlCl₂(THF)₄]⁺ species have all been observed, and the influence of temperature, concentration, and solvent on structure has been studied. Means et al.[4] obtained only [AlCl₄][AlCl₂(THF)₄] ionic crystals from a 1:2 mole ratio of AlCl₃ and THF in toluene, while Cowley et al.[3] obtained molecular AlCl₃·2THF crystals, from dissolution of (Me₂N)₃SiCl·AlCl₃ in THF. Derouault and Forel[1] also obtained ionic crystals of [AlCl₄][AlCl₂(THF)₄] from a saturated solution of AlCl₃ in THF, and also showed that [AlCl₄][AlCl₂(THF)₄] could easily lose THF in vacuo at room temperature, in the solid state, to yield a 1:1 complex [AlCl₄][AlCl₂(THF)₄] → 2AlCl₃·THF + 2THF.

In this paper, we present the results of a ^{27}Al magic-angle sample-spinning (MASS) NMR study on solid-state AlCl₃–THF complex systems and interpret our chemical shift and quadrupole coupling constant data in structural terms, which may be of general interest.

Experimental Section

Sample Preparation. Reagent grade anhydrous Al₂Cl₆ (13.7 g, 51.4 mmol) was transferred to 137 mL of dry toluene in a 250-mL round-bottomed flask. An 18.0-mL portion of dry THF (0.207 mol) was then added, and the mixture was heated to 100 °C for 2 h under 1 atm of N₂. One portion of the product was kept at −18 ± 2 °C, and a second portion was kept at 1 ± 1 °C for about 10 h, after initial cooling to room temperature. Colorless crystals were obtained from both batches.

Crystals deposited at 1 °C had a stepped-pyramidal shape and were ~7 × 7 mm at the base of the pyramid, while crystals made at −18 °C were much smaller and did not have any noticeable shape. Both sets of crystals were filtered off under N₂, and a portion of each sample was stored at −18 °C. The remainder of each sample was then kept at room temperature under N₂. The history of samples A–D can be summarized as follows: sample A was crystallized at −18 °C and kept at room temperature; sample B was crystallized at 1 °C and then kept at room temperature; sample C was crystallized at −18 °C and kept at −18 °C; sample D was crystallized at 1 °C and kept at −18 °C. We prepared AlCl₃·THF (sample F and a portion of sample E) by heating samples A or D at 57 °C for 5 h at ~0.1 Torr.

Nuclear Magnetic Resonance Spectroscopy. ^{27}Al MASS NMR spectra were obtained at 8.45 and 11.7 T using "home-built" spectrometers, which consist of Oxford Instruments (Osney Mead, Oxford, U.K.) 8.45-T 89-mm-bore or 11.7-T 52-mm-bore superconducting solenoid magnets, Nicolet Instrument Corp. (Madison, WI) Model 1280 computers for data acquisition, and Amplifier Research (Souderton, PA) Model 200L amplifiers for final radio frequency pulse generation. MASS NMR spectra were obtained by using a home-built probe equipped with a "Windmill"-type spinner. Samples were spun in the 6–7.5-kHz range, with less than 20 Hz of fluctuation. Chemical shifts are reported in ppm from external standards of 1 M Al(H₂O)₆Cl₃ aqueous solutions. More positive values correspond to low-field, high-frequency, paramagnetic or deshielded values (IUPAC δ scale). Line broadenings due to exponential multiplication were 100–200 Hz, depending on the line width.

Results and Discussion

The ^{27}Al MASS NMR spectra of samples A–D at 11.7 and 8.45 T clearly show different spectra, dependent upon sample history. For example, sample D has a main second-order powder pattern, while samples A and B have two major peaks together with numerous spinning side bands, and sample C appears to be a superposition of the spectra of samples A (or B) and D (Figure 1). The chemical shift of the resonance at ~103 ppm is field independent, and the peak has numerous first-order quadrupolar

(1) Derouault, J.; Forel, M. T. *Inorg. Chem.* **1977,** *16,* 3207.
(2) Derouault, J.; Granger, P.; Forel, M. T. *Inorg. Chem.* **1977,** *16,* 3214.
(3) Cowley, A. H.; Cushner, M. C.; Davis, R. E.; Riley, P. E. *Inorg. Chem.* **1981,** *20,* 1179.
(4) Means, N. C.; Means, C. M.; Bott, S. G.; Atwood, J. L. *Inorg. Chem.* **1987,** *26,* 1466.
(5) Bach, B.; Ubbelohde, A. R. *Proc. R. Soc. London, A* **1971,** *325,* 437. Bach, B.; Ubbelohde, A. R. *J. Chem. Soc. A* **1971,** 3669.